



Optimal State Feedback Control for Bicycle Stabilization Using APT-FPSO Algorithm

Mana Azim Araghi ^a, Seyed Mohammad Nami Mir Mohammad Sadeghi ^b,
Seyed Ali Mir Mohammad Sadeghi ^{c,*}

^a Faculty of New Technologies Engineering, Shahid Beheshti University, Tehran, Iran

^b Faculty of New Sciences & Technologies, University of Tehran, Tehran, Iran

^c Department of Mechanical Engineering, Virginia Tech, Blacksburg

Received 13 February 2022; Accepted 16 March 2022

Abstract

Advanced control systems are required to maintain bicycle stability due to its unstable open-loop behaviour. This work is aimed at designing an optimal state feedback control system for bicycle stabilization. The performance index of the optimal control system is minimized using the newly developed adaptive particularly tunable fuzzy particle swarm optimization algorithm. The states of the system are estimated using a state observer. The obtained results are compared with those of the linear-quadratic regulator (LQR). The main advantage of the developed control system is that, unlike the LQR controller that is limited to linear systems, it can be extended to nonlinear control systems.

Keywords: Bicycle Stabilization, State Observer, Optimal Control, APT-FPSO Algorithm

1. Introduction

Bicycles are one of the most popular ways to travel due to their entertainment value, environmental friendliness, and health benefits. However, the bicycles' safety has always been an important issue since their debut. Novice bicyclists usually have difficulty controlling the bicycle due to unstable open-loop behavior. Therefore, bicycle stabilization has been a challenging problem for control engineers.

A basic bicycle consists of four linked rigid bodies which have a symmetry plane [1]. The four main parts of a bicycle consists of two wheels that are placed behind each other, and the rear and front frame, to which the wheels are connected by revolute joints and that are interconnected by a vertical or inclined hinge [2]. For bicycles with more restricted steer rate and steer angle, the value iteration controller performs slightly better than the linear quadratic regulator (LQR) controller. For

bicycles with less restrictive actuator limits, the LQR and value iteration controller have almost equivalent Basin Widths [3]. Findlay et al. Analyzed the use of front wheel steering input for controlling the bicycle roll angle [4]. Sanjurjo et al. accentuated the importance of roll angle in the stability of bicycles [5]. Using a wheel speed sensor and three angular rate sensors, they developed a roll angle estimator based on the Kalman filter. Cui et al. [6] took advantage of two control strategies to maintain an autonomous bicycle's stability while moving. First, the steering angle was set to zero, and the bicycle stabilization was performed using a flywheel. Second, the flywheel was turned off, and the bicycle was balanced through the handlebar. Schwab et al. [7] have developed a model for describing bicycle control while steering and stabilizing a bicycle. The feedback gains of their control model were used to identify the specific optimal control linear-quadratic regulator (LQR) cost function. M. Baquero-Suarez et al. [8] offered a two-stage observer-based

* Corresponding Author. Email: alimmsadeghi@vt.edu

feedback control strategy to stabilize a riderless bicycle in its upright position. They assumed that the bicycle was moving forward at a constant speed.

Intelligent, meta-heuristic optimization algorithms have been widely used to solve optimal control problems [9, 10]. MirMohammadSadeghi et al. have used four optimization algorithms to optimally tune PID gains of an automotive engine idle speed [11].

Bakhshinezhad et al. have recently developed a modified version of the particle swarm optimization algorithm (PSO) called adaptive particularly tunable fuzzy particle swarm optimization (APT-FPSO) algorithm [12]. In this algorithm, a fuzzy inference system updates the personal and global learning coefficients for each particle individually within each iteration. Statistical evidence has been provided to confirm enhanced exploitation ability of APT-FPSO compared to the standard PSO. Many studies have used the APT-FPSO algorithm to surmount complicated engineering optimization problems [13, 14].

In this paper, an optimal control system is developed for bicycle stabilization. APT-FPSO algorithm minimizes the performance index of the optimal control problem in order to find the optimal state feedback gain. The performance index is expressed such that in addition to the control energy (steering torque) the system's states (roll and steering angles) are minimized to zero (zero tracking control problem). The contribution of this paper is twofold. Firstly, the bicycle is stabilized by an optimal controller optimized using a metaheuristic algorithm, in which the states of the controlled system are estimated using a state observer. Second, this would be the first time the APT-FPSO algorithm is tailored to solve an optimal control problem.

2. Modeling

Fig. 1 shows the free body diagram of the bicycle consisting of four rigid bodies. The front frame that consists the front fork and handlebar, the rear frame, the rear wheel, and the front wheel. The wheels in this model are assumed to be narrow with a zero-slip assumption between contact surfaces. The basic model of the bicycle has two degrees of freedom: the roll rate of rear frame ($\dot{\varphi}$) and the steering rate ($\dot{\delta}$). Bicycle lateral motion is described by a second-order differential equation as follows [10].

$$M\ddot{\mathbf{x}} + [vC_1]\dot{\mathbf{x}} + [gK_0 + v^2K_2]\mathbf{x} = \mathbf{u} \quad (1)$$

In this equation, v is forward speed and q described the degrees of freedom $\mathbf{x} = [\varphi \ \delta]^T$, and \mathbf{u} is the tilting torque (T_φ) and the handlebar torque (T_δ). M , C_1 , K_0 and K_2 are derived according to [15].

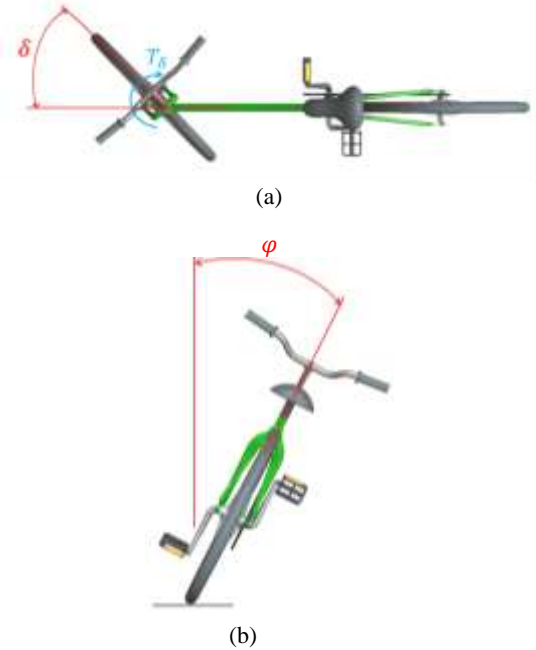


Fig. 1. The bicycle degrees of freedom.

3. Control Systems Design

This section discusses the developed control system. Before proceeding to discuss the developed control system, the linear quadratic regulator (LQR) controller, the state observer, and the APT-FPSO are overviewed.

3.1. Overview of LQR Controller

LQR is an optimal control system based on state-space representation of a dynamical system. The LQR structure feeds back the full state vector, then multiplies it by a gain matrix K and subtracts it from the scaled reference. In this solution, the optimal K matrix is found by choosing closed-loop characteristics, especially how well the system performs, rather than finding the poles' locations. As shown below, a cost function is set up that adds up the weighted sum of performance and the control effort over the entire time span.

$$J = \int_{t_0}^{t_f} (\mathbf{x}^T Q \mathbf{x} + \mathbf{u}^T R \mathbf{u}) dt \quad (2)$$

Where Q and R are, respectively, the weight matrices for states and the input. The weight matrices Q and R must be positive definite and positive semi-definite, respectively.

The LQR method finds a deterministic solution for the above optimization problem in the form of a state feedback gain matrix ($U = -Kx$), subject to the system dynamics: $\dot{x} = Ax + Bu$.

$$\begin{aligned} \dot{x} &= A_{OL}x + Bu \\ &= (A_{OL} - KB)x = A_{CL}x \end{aligned} \quad (3)$$

Where the subscripts OL and CL stand for open-loop and closed-loop, respectively. The gain matrix K is found to be:

$$K = R^{-1}B^T P(t) \quad (4)$$

where $P(t)$ is the solution to the Riccati differential equation:

$$A^T P(t) + P(t)A - P(t)BR^{-1}B^T P(t) = \dot{P}(t) \quad (5)$$

In the special case of having an infinite horizon ($t_f \rightarrow \infty$), it can be proved that $P(t)$ is constant, and the problem then becomes an algebraic Riccati equation as shown below:

$$A^T P(t) + P(t)A - P(t)BR^{-1}B^T P(t) = 0 \quad (6)$$

3.2. State Observer Design

Access to the internal states of a system is crucial for many control system applications [16]. In the state feedback controllers, for instance, the control effort is obtained by multiplying a gain matrix to the system's internal states. However, in most practical applications, the system's internal states are not accessible. By using the inputs and outputs of a system, a state observer estimates its internal states. Fig 2. depicts the block diagram of a real system and a state observer.



Fig. 2. The state observer system.

A state observer is a dynamic system with the following state and output equations:

$$\begin{aligned} \dot{\hat{x}} &= A\hat{x} + Bu + L(y - \hat{y}) \\ \hat{y} &= C\hat{x} + Du \end{aligned} \quad (7)$$

where \hat{x} and \hat{y} are estimations of x and y , respectively. The gain matrix L is called *Luenberger* matrix, and $L(y - \hat{y})$ is a correction term added to the observer state equation. Substituting the output equation into the state equation of the observer and simplifying the resulting yield:

$$\begin{aligned} \dot{\hat{x}} &= A\hat{x} + Bu + Ly - L(C\hat{x} + Du) \\ &= (A - LC)\hat{x} + [B - LD \quad L] \begin{bmatrix} u \\ y \end{bmatrix} \end{aligned} \quad (8)$$

According to Eq. 8, the matrix $\begin{bmatrix} u \\ y \end{bmatrix}$ is the state observer input formed by augmenting the input and output of the real system. Based on Eq. 7, the error dynamics can be written as:

$$\begin{aligned} \dot{e} &= \dot{x} - \dot{\hat{x}} \\ &= (A - LC)e \end{aligned} \quad (9)$$

Zero convergence of the estimation error entails the stable equilibrium point to be zero. To this end, the matrix L should be selected so that $A-LC$ is stable, i.e., it has all the eigenvalues inside the unit circle. MATLAB place command can be used to find the matrix L that replaces the eigenvalues of $A-LC$ with the observer desired poles.

3.3. Overview of APT-FPSO Algorithm

The adaptive particularly tunable fuzzy particle swarm optimization (APT-FPSO) algorithm is an enhanced version of the Particle swarm optimization (PSO) with the improved exploitation ability [17]. Using fuzzy membership functions, this algorithm updates each particle's global and personal learning coefficients individually at each iteration. The APT-FPSO algorithm steps can be described as follow:

- 1) Dedicate a random position in the search space to each particle: the Initialization step,
- 2) Appraise the fitness of each of the particles.
- 3) For each particle, compare the fitness value of the current position with the personal best position (*pbest*). If the current value is better than *pbest*, replace *pbest* with the current position; then, for each of the particles, compare *pbest* with global best position (*gbest*). If the current *pbest* is better than *gbest*, replace *gbest* with *pbest*.
- 4) Update the personal and global learning coefficients for each particle with respect to their normalized fitness value and iteration number.
- 5) Update each particle's position and velocity with respect to their *pbest* and the *gbest*.
- 6) Repeat stages 3 to 5 until a termination criterion is met.

In this algorithm, the position and velocity of the i^{th} particle at the t^{th} generation will be found by (10) and (11).

$$x_{t+1}^i = x_t^i + v_{t+1}^i \quad (10)$$

$$v_{t+1}^i = w_i \times v_t^i + c_{1,t}^i \times r1 \times (p_t^i - x_t^i) + c_{2,t}^i \times r2 \times (p_t^g - x_t^i), \quad (11)$$

Where p_t^i is the personal best position of the i^{th} particle in the t^{th} iteration, and p_t^g indicates the global best in the t^{th} iteration. In addition, $r1$ and $r2$ are two uniformly distributed random numbers within $[0, 1]$. w_i , $c_{1,t}^i$, and $c_{2,t}^i$ denote, respectively, inertia weight, personal, and global learning coefficients for the i^{th} particle at the t^{th} generation [18]. At each iteration, the designed fuzzy inference system (FIS) is evaluated for each particle. The inputs to the FIS are normalized iteration (NI t) and normalized fitness index (NFI). These inputs are fuzzified using three linguistic variables and Gaussian membership functions (MFs). The outputs of the FIS are $c_{1,t}^i$ and $c_{2,t}^i$ that are defuzzified by five triangular MFs. For further elaborations on the APT-FPSO algorithm, please refer to [12, 19].

3.4. APT-FPSO-Based Optimal State Feedback Control System

This section explains the development of the APT-FPSO-based optimal state feedback control system. The plant under control is a bicycle that is moving with a constant forward velocity. The problem is defined in the form of a state feedback control system. Thus, the control input (steering torque) is obtained by multiplying a gain to the internal states of the system and subtracting it from the reference input ($u = r - K\hat{x}$). A state observer is designed to estimate the internal states of the system (bicycle roll and steering angles). Based on the plant's and state observer's dynamic systems, discussed previously, the state space representation of these two systems augmented together can be written as follows

$$\begin{bmatrix} \dot{x} \\ \dot{\hat{x}} \end{bmatrix} = \begin{bmatrix} A & -BK \\ LC & A - BK - LC \end{bmatrix} \begin{bmatrix} x \\ \hat{x} \end{bmatrix} + \begin{bmatrix} B \\ B \end{bmatrix} r \quad (12)$$

$$y = [C \quad -DK] \begin{bmatrix} x \\ \hat{x} \end{bmatrix} + Dr$$

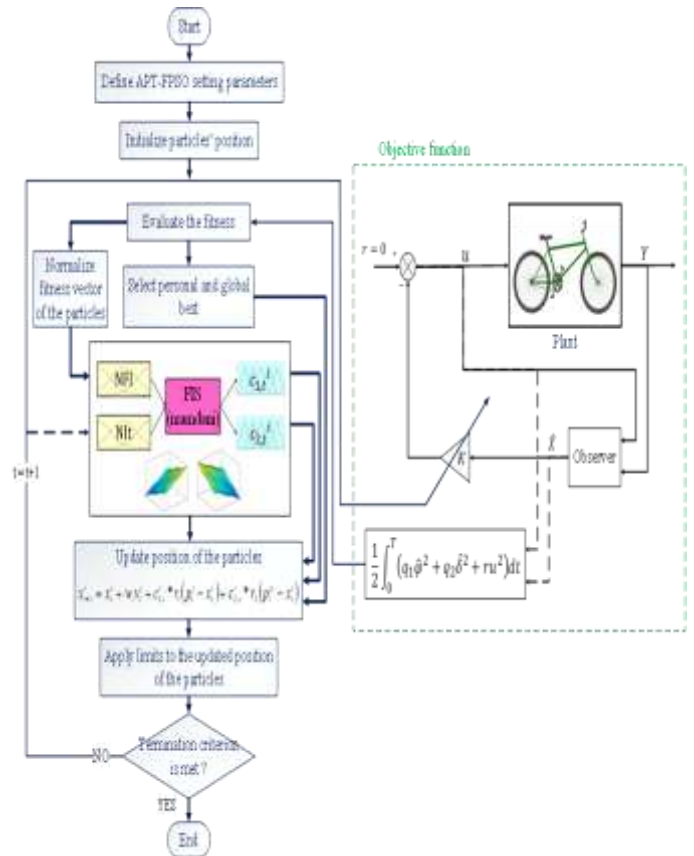


Fig. 3. APT-FPSO-based optimal state feedback control system.

Fig. 3 shows the flowchart of the developed optimal state feedback control system. As can be seen, the observer estimates the internal states of the bicycle model. Then, the APT-FPSO algorithm finds the optimal feedback gain by minimizing the performance index. For the optimal control problem, a quadratic cost function is set to allow the system states to track zero and to minimize the control energy. In other words, APT-FPSO finds the optimal controller gains via the minimization of the performance index such that the estimated state of the system and the input control effort are minimized.

4. Results and Discussions

In this section, the simulation details, in addition to the obtained results, are discussed. The forward velocity of the bicycle is set to 7 m/s. Control input reference is set equal to zero since the purpose of the control system is to maintain the internal states of the system at zero. Besides, the bicycle is initially released with five degrees of roll angle ($\varphi_0 = 5^\circ$). The observer desired poles are set equal to $[-4 \ -5 \ -6 \ -7]$. Regarding the performance index of both the LQR controller and the developed control system, $Q = [10 \ 5]$ and $R = 1$.

For the APT-FPSO algorithm, the size of the population and the maximum number of iterations were set to 25 and 100, respectively.

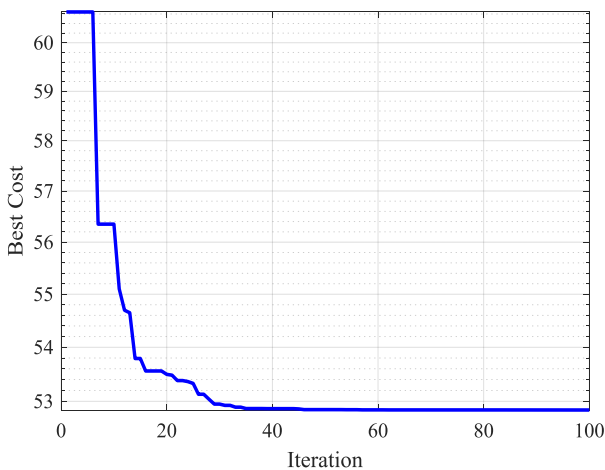


Fig. 4. Minimization of the Cost Function Over the Number of iterations

Additionally, for the decision variables $\mathbf{K} = [k_1 \ k_2 \ k_3 \ k_4]$ the lower and upper bounds were, respectively, set to be $[-15 \ -5 \ -10 \ -5]$ and $[15 \ 5 \ 10 \ 5]$.

Fig 4. depicts the convergence of the cost value minimized by the APT-FPSO algorithm. As can be seen, the algorithm converges to the minimum value after 30 iterations.

Fig. 5 shows the response of the closed-loop control system. The solid green line is the ideal response obtained by solving the differential equations of motion for the system using the MATLAB *lsim* command. In practice, however, the states of a system cannot be obtained unless using an observer/estimator. The black dot-dash line is the observer's estimate of the state of the system. The observer dynamic response depends on the places of the observer's desired poles. According to Figure 5, the controller stabilizes the bicycle by rotating the steering wheel in the same direction as the initial roll angle. The solid blue line illustrates the input control effort, i.e., the steering wheel torque. Besides, it can be seen that after 3 seconds, the controller settles the states to zero. The true roll angle starts from the initial condition $\varphi_0 = 5^\circ$, yet the state estimator starts from zero and estimates the states in less than 0.5 sec.

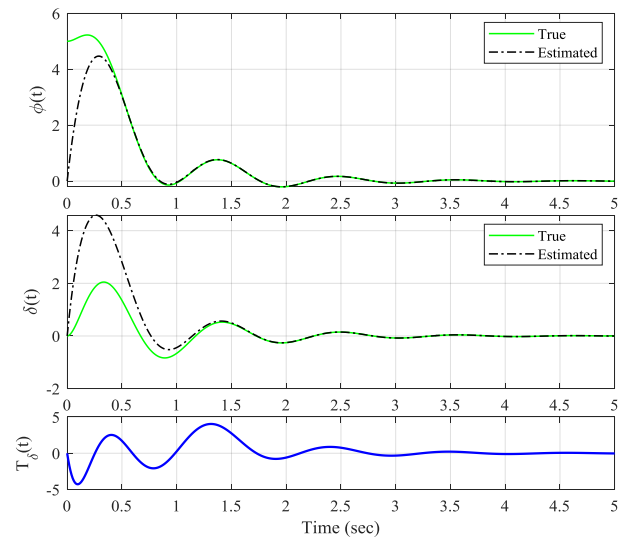


Fig. 5. The Closed-Loop System Response

The developed control system is compared with the LQR controller in Fig 6. It can be seen that the designed control system settles to the equilibrium point more rapidly than the LQR controller. In other words, with regards to the states $\mathbf{x} = [\varphi \ \delta]^T$, the presented method has improved the settling time compared to the LQR. However, this has resulted to more oscillations and more control energy. The developed control system used a *meta-heuristic*

optimization algorithm to determine the control input u , in contrast to the LQR controller that finds the optimum solution deterministically. In this sense, the solution offered by the developed controller may be deemed sub-optimal when compared to the LQR controller. Therefore, the developed control system may not outperform the LQR controller for linear dynamic systems when considering the control energy. The results of the two controllers are compared here to assess the performance of the developed control system. However, the performance of the LQR controller is limited to *linear* systems. Therefore, the advantage of the developed control system over the LQR controller lies in its ability to surmount control problems with *nonlinear* dynamic plants.

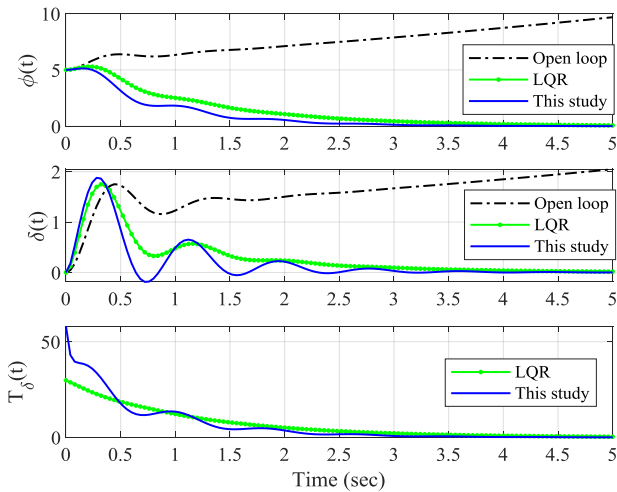


Fig. 6. Comparison of the controller developed in this study with the LQR controller.

Fig. 7 illustrates and compares the phase-plane diagram of the system's states in the open-loop and closed-loop conditions. This diagram illustrates the rate of the states with respect to the states, and it is used to demonstrate the system's stability. In this diagram, the states depart from the initial conditions, arrive at the zero point for stable systems, and diverge to infinity for unstable systems. Accordingly, the states of the closed-loop systems (solid blue and green lines) depart from the initial conditions and arrive at the stable equilibrium point. On the contrary, the states of the unstable open-loop system (black dot-dash line) depart from the initial condition but diverge towards infinity.

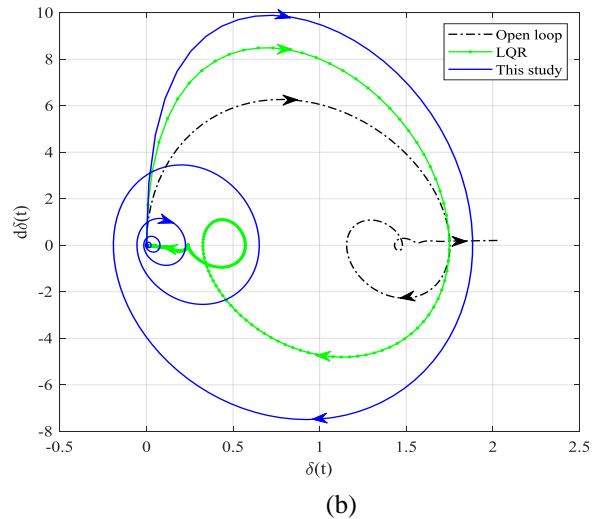
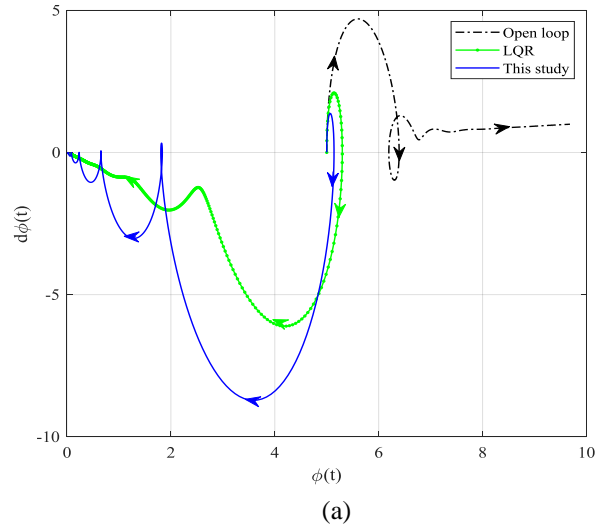


Fig. 7. Phase plane diagram of the systems states.

5. Conclusion

In this paper, we developed an optimal state feedback control system for bicycle stabilization. A state observer has been utilized to estimate the system's internal states. The performance index of the optimal control problem was minimized using the newly developed APT-FPSO algorithm. The performance of the developed control system was compared with that of the LQR controller. It was observed that the developed control system successfully stabilized the unstable open-loop system of the bicycle. In addition, the state estimator could estimate the system's state in less than 0.5 sec. Moreover, the controller could settle the states to zero (reference level) in 3 seconds.

The state estimator and the controller are amenable for real-time implementation due to their fast performance. Unlike the LQR controller, the developed control system could be extended to solve nonlinear optimal control problems.

References

- [1] J. M. Papadopoulos, R. S. Hand, and A. Ruina, "Bicycle and motorcycle balance and steer dynamics," *I. Linearized equations of lateral motion for a simple model [C]. Cornell University*, 1990.
- [2] A. L. Schwab and J. P. Meijaard, "A review on bicycle dynamics and rider control," *Vehicle system dynamics*, vol. 51, no. 7, pp. 1059-1090, 2013.
- [3] D. Meehan and A. Ruina, "Linear and nonlinear controllers of an autonomous bicycle have almost identical basins of attraction in a non-linear simulation," 2020: Symposium on the Dynamics and Control of Single Track Vehicles.
- [4] C. Findlay, J. Moore, and C. Perez-Maldonado, "SISO control of a bicycle-rider system," *mh*, vol. 1, p. 2, 2006.
- [5] E. Sanjurjo, M. A. Naya, J. Cuadrado, and A. L. Schwab, "Roll angle estimator based on angular rate measurements for bicycles," *Vehicle system dynamics*, 2018.
- [6] L. Cui *et al.*, "Nonlinear Balance Control of an Unmanned Bicycle: Design and Experiments," in *2020 IEEE/RSJ International Conference on Intelligent Robots and Systems (IROS)*, 2020, pp. 7279-7284: IEEE.
- [7] A. L. Schwab, J. Meijaard, and J. Kooijman, "Lateral dynamics of a bicycle with a passive rider model: stability and controllability," *Vehicle system dynamics*, vol. 50, no. 8, pp. 1209-1224, 2012.
- [8] M. Baquero-Suárez, J. Cortés-Romero, J. Arcos-Legarda, and H. Coral-Enriquez, "A robust two-stage active disturbance rejection control for the stabilization of a riderless bicycle," *Multibody System Dynamics*, vol. 45, no. 1, pp. 7-35, 2019.
- [9] K. Nikzadfar, N. Bakhshinezhad, S. A. MirMohammadSadeghi, H. T. Ledari, and A. Fathi, "An Optimal Gear Shifting Strategy for Minimizing Fuel Consumption Based on Engine Optimum Operation Line," SAE Technical Paper0148-7191, 2019.
- [10] S. Mir Mohammad Sadeghi, S. Hoseini, A. Fathi, and H. Mohammadi Daniali, "Experimental Hysteresis Identification and Micro-position Control of a Shape-Memory-Alloy Rod Actuator," *International Journal of Engineering*, vol. 32, no. 1, pp. 71-77, 2019.
- [11] S. A. MirMohammadSadeghi, K. Nikzadfar, N. Bakhshinezhad, and A. Fathi, "Optimal Idle Speed Control of a Natural Aspirated Gasoline Engine Using Bio-inspired Meta-heuristic Algorithms," *International Journal of Automotive Engineering*, vol. 8, no. 3, pp. 2792-2806, 2018.
- [12] N. Bakhshinezhad, S. Mir Mohammad Sadeghi, A. Fathi, and H. Mohammadi Daniali, "Adaptive particularly tunable fuzzy particle swarm optimization algorithm," *Iranian Journal of Fuzzy Systems*, vol. 17, no. 1, pp. 65-75, 2020.
- [13] A. Mirmohammad Sadeghi, A. Amirkhani, and B. Mashadi, "Braking intensity recognition with optimal K-means clustering algorithm," *Journal of Computational & Applied Research in Mechanical Engineering (JCARME)*, 2021.
- [14] M. N. Gilvaei, H. Jafari, M. J. Ghadi, and L. Li, "A novel hybrid optimization approach for reactive power dispatch problem considering voltage stability index," *Engineering Applications of Artificial Intelligence*, vol. 96, p. 103963, 2020.
- [15] J. P. Meijaard, J. M. Papadopoulos, A. Ruina, and A. L. Schwab, "Linearized dynamics equations for the balance and steer of a bicycle: a benchmark and review," *Proceedings of the Royal society A: mathematical, physical and engineering sciences*, vol. 463, no. 2084, pp. 1955-1982, 2007.
- [16] S. F. Hoseini, S. A. MirMohammadSadeghi, A. Fathi, and H. M. Daniali, "Adaptive predictive control of a novel shape memory alloy rod actuator," *Proceedings of the Institution of Mechanical Engineers, Part I: Journal of Systems and Control Engineering*, vol. 235, no. 3, pp. 291-301, 2021.
- [17] S. A. M. Sadeghi, B. Ebrahimpour, N. Bakhshinezhad, and S. M. N. M. M. Sadeghi, "Analytical solution of nonlinear Van der Pol oscillator using a hybrid intelligent analytical inverse method," *Turkish Journal of Computer and Mathematics Education (TURCOMAT)*, vol. 12, no. 13, pp. 5614-5625, 2021.
- [18] A. Farjoud, M. Craft, W. Burke, and M. Ahmadian, "Experimental investigation of MR squeeze mounts," *Journal of Intelligent Material Systems and Structures*, vol. 22, no. 15, pp. 1645-1652, 2011.
- [19] S. MirMohammad Sadeghi, N. Bakhshinezhad, A. Fathi, and H. Mohammadi Daniali, "An Optimal Defect-free Synthesis of Four-bar Mechanisms by Using Constrained APT-FPSO Algorithm," *Journal of Computer & Robotics*, vol. 12, no. 2, pp. 39-48, 2019.